Acta Cryst. (1990). B46, 629–637

Structural Variations in 3,4-Dihydro-2*H*-pyran Ketals: Acyl and Aryl Warfarin Derivatives

BY GERARD RUGGIERO, ANSON LEE THAGGARD AND EDWARD J. VALENTE

Department of Chemistry, Mississippi College, Clinton, MS 39058, *USA*

AND DRAKE S. EGGLESTON

Department of Physical and Structural Chemistry, Smith, Kline & French Laboratories, King of Prussia, PA 19406, *USA*

(*Received* 18 *August* 1989; *accepted* 15 *March* 1990)

Abstract

The crystal structures of (±)-*cis*-2-methyl-5-oxo-4-phenyl-3,4-dihydro-2*H*,5*H*-pyrano[3,2-*c*][1]benzopyran-2-yl acetate [$C_{21}H_{18}O_5$, M_r = 350·37, monoclinic, $P2_1/n$, a = 12·091 (4), b = 8·288 (3), c = 17·840 (5) Å, β = 106·34 (2)°, V = 1715 (2) Å^3, Z = 4, D_x = 1·356 g cm^{-3}, λ(Mo $K\bar{\alpha}$) = 0·7107 Å, μ = 0·904 cm^{-1}, $F(000)$ = 736, T = 295 K, R = 0·050 for 2767 observations with $I \geq 3\sigma(I)$] and (6*R*,12*S*)-(−)-6,8-dimethyl-6,12-methano-6*H*,12*H*,13*H*-[1]benzopyran[4,3-*d*][1,3]benzodioxocin-13-one [$C_{20}H_{16}O_4$, M_r = 320·36, tetragonal, $P4_3$, a = 10·788 (4), c = 13·587 (9) Å, V = 1581 (2) Å^3, Z = 4, D_x = 1·345 g cm^{-3}, λ(Mo $K\bar{\alpha}$) = 0·7107 Å, μ = 0·873 cm^{-1}, $F(000)$ = 672, T = 295 K, R = 0·049 for 1425 observations with $I \geq 2{\cdot}5\sigma(I)$] are described. They are acyl and aryl ketals of warfarin, respectively, and contain an embedded dihydropyran ring. The molecules were studied as part of a series of axial 2-O-substituted-2-methyl-3,4-dihydro-2*H*-pyran structures which show (hemi)ketal C—O bond-length variations indentified through factor analysis with the systematic geometrical changes associated with a spontaneous elimination (*E*1-like) reaction from the ketal leading to 2-methyl-4*H*-pyran. As in α-tetrahydropyranyl acetals, the C—O lengths in dihydropyranyl ketals can be expressed as a function of the electron-withdrawing ability of the substituent conjugate base, and the slopes of the relationships for the two systems are similar. Corresponding endocyclic C—O lengths are about 0·052 Å longer in these model dihydropyranyl ketals.

Introduction

The analysis of molecular dynamics from solid-state structures produces useful insights into reaction mechanisms and conformational motions (Bürgi & Dunitz, 1983). A particularly relevant example is the study of the stereochemical preferences associated with the 'anomeric effect'. Variations in the ground-state structures of a series of tetrahydropyranyl acetals, determined from crystal structures, show systematic geometrical changes as a function of the electron-withdrawing ability of the exocyclic leaving group (Briggs, Glenn, Jones, Kirby & Ramaswamy, 1984), which for the axial anomers correlate simply with kinetic data for their hydrolysis (Allen & Kirby, 1984). The path of the changes has been interpreted as a model for spontaneous acetal cleavage, complete with estimates of the activation energy and geometry of the transition state (Bürgi & Dubler-Steudle, 1988). Such an analysis provides a satisfying experimental confirmation of the relationship between structure and chemical reactivity, and demonstrates the ability of the approach to extract information in accord with sound chemical mechanistic intuition.

Our attention also has been drawn to an anomeric system as part of a structural study on the conformation of the heterocycle 3,4-dihydro-2*H*-pyran. We have focused on a series of compounds similar to the anticoagulant drug and rodenticide warfarin. Warfarins exist in solution in a dynamic equilibrium between two diastereomeric and anomeric hemiketals, which incorporate the dihydropyran ring, and an intermediate open form (Valente, Lingafelter, Porter & Trager, 1977). They crystallize most commonly as one of the cyclic hemiketals. We have examined the solid-state structures of more than 30 of these warfarin hemiketals and their closely-related methyl ketal derivatives. In general, the endocyclic and exocyclic C—O bonds in the (hemi)ketals of the embedded dihydropyran ring show significant deviations from the norm (1·42–1·43 Å; Sutton, 1965). An explanation invoking contributions to the ground state from likely resonance structures has been offered (Valente, Santarsiero & Schomaker, 1979), analogous to the charge-separation model advanced for the tetrahydropyranyl acetals (Briggs, Glenn, Jones, Kirby & Ramaswamy, 1984). A cursory comparison of the C—O lengths between the axial 2-O-

0108-7681/90/050629-09$03.00

© 1990 International Union of Crystallography

substituted dihydropyrans and examples of corresponding saturated heterocycles suggested that the endocyclic C—O linkage of the dihydropyrans is, however, significantly longer.

To examine in more detail the structural features of the dihydropyranyl ketals and the influences on the disparate endocyclic and exocyclic C—O lengths by 2-O-substituents, we have prepared warfarin derivatives with ketal substituents having differing leaving-group tendencies. A mechanistic explanation for the systematic structural changes in the series is then sought through factor analysis. In the present work, we examine the molecular structures of a 2-O-acyl (I) and a 2-O-aryl (II) warfarin ketal, extending the range of potential leaving groups among ketal structures in the anomeric 2-substituted dihydropyran system. In each, the dihydropyran ring is fused at its unsaturation with a benzopyranone system, and its 2-O-substitutents are axial. The results are compared with the spontaneous cleavage in related tetrahydropyranyl acetals.

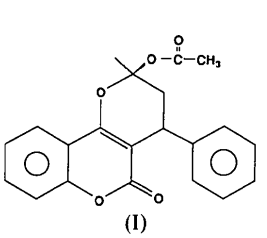

(I)

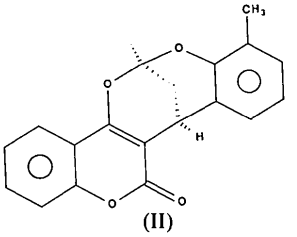

(II)

Experimental

Warfarins are made by Michael-type addition of unsaturated ketones with 4-hydroxycoumarin (Ikawa, Stahmann & Link, 1944). Intermediate 2-ethanoylwarfarin (I) results from brief reaction of warfarin, ethanoic anhydride and perchloric acid (Seidman, Robertson & Link, 1950) and crystallizes from 2-propanol as plates, m.p. 477–478 K. Longer reaction times result in a ring-dehydrated warfarin, 2-methyl-4-phenyl-4*H*,5*H*-pyrano[3,2-*c*][1]benzopyran-5-one. Persulfate oxidation of 2,6-dimethylanisole by a modified procedure based on Carter & Wallace (1983) produces 2-methoxy-3-methylbenzaldehyde, which through the Michael addition results in 2′-methoxy-3′-methylwarfarin. Resolution of this compound with (+)-quinidine and deprotection of the isomer from the less soluble (in acetone) salt with hydroiodic/glacial acetic acids forms (*S*)-2′-hydroxy-3′-methylwarfarin but this compound spontaneously undergoes an intramolecular cyclic dehydration to form (II); crystals from methanol, m.p. 477–478 K. Specimens, (I) 0·30 × 0·35 × 0·20 mm, and (II) 0·20 × 0·20 × 0·70 mm were chosen for data collection on a CAD-4 diffractometer. The lattice type was deduced from oscillation photographs and cell constants were derived from 25 accurately centered higher-order intensities, $30 \le 2\theta \le 35°$. At 295 K for racemic (I), the cell is monoclinic, space group $P2_1/n$ ($h0l$ absent for $h + l$ odd, $0k0$ absent for k odd) and the cell constants are a = 12·091 (4), b = 8·288 (3), c = 17·840 (5) Å, β = 106·34 (2)°. At 295 K for resolved (II), the cell is tetragonal, space group $P4_3$ ($00l$ absent for $l \neq 4n$, *S* isomer) and the cell constants are a = 10·788 (4), c = 13·587 (9) Å.

Table 1. *Positions and equivalent isotropic vibrational amplitudes for the non-*H *atoms in* (I), *with e.s.d.'s in parentheses*

$B_{eq} = (8\pi^2/3)\sum_i\sum_j U_{ij} a_i^* a_j^* \mathbf{a}_i.\mathbf{a}_j.$

	x	y	z	B_{eq}(Å^2)
O1	0·87863 (11)	0·7440 (2)	0·44386 (7)	3·96 (3)
O2	0·77897 (14)	0·7272 (2)	0·32013 (8)	5·18 (4)
O3	0·76105 (11)	0·3024 (2)	0·49399 (7)	3·83 (3)
O4	0·56896 (11)	0·2864 (2)	0·44982 (7)	3·57 (3)
O5	0·45024 (13)	0·1059 (2)	0·37230 (10)	5·67 (4)
C2	0·8024 (2)	0·6625 (2)	0·38299 (10)	3·45 (4)
C3	0·75788 (14)	0·5090 (2)	0·39969 (9)	3·02 (4)
C4	0·79391 (14)	0·4474 (2)	0·47216 (10)	3·02 (3)
C5	0·9090 (2)	0·4766 (3)	0·61255 (11)	4·10 (4)
C6	0·9822 (2)	0·5696 (3)	0·66964 (11)	4·97 (5)
C7	1·0197 (2)	0·7178 (3)	0·65093 (12)	4·84 (5)
C8	0·9854 (2)	0·7759 (3)	0·57567 (13)	4·47 (5)
C9	0·9121 (2)	0·6820 (2)	0·51831 (10)	3·34 (4)
C10	0·87332 (14)	0·5331 (2)	0·53548 (10)	3·20 (4)
C11	0·6776 (2)	0·4171 (2)	0·33331 (9)	3·37 (4)
C12	0·6804 (2)	0·2392 (2)	0·35668 (11)	3·73 (4)
C13	0·6728 (2)	0·2138 (2)	0·43865 (11)	3·62 (4)
C14	0·6876 (2)	0·0412 (3)	0·46746 (14)	5·25 (6)
C15	0·5555 (2)	0·4872 (3)	0·30618 (10)	3·46 (4)
C16	0·5196 (2)	0·6174 (3)	0·34187 (11)	4·13 (4)
C17	0·4076 (2)	0·6770 (3)	0·31551 (14)	5·41 (6)
C18	0·3299 (2)	0·6041 (3)	0·25303 (14)	5·88 (6)
C19	0·3645 (2)	0·4763 (3)	0·21611 (14)	5·92 (6)
C20	0·4769 (2)	0·4178 (3)	0·24157 (12)	4·69 (5)
C21	0·4643 (2)	0·2242 (3)	0·41270 (12)	3·97 (4)
C22	0·3702 (2)	0·3235 (3)	0·42747 (13)	4·80 (5)

Intensity data were measured to $2\theta = 60°$ using variable speed ω–θ scans; for (I) (h 0–17, k 0–11, l −25 to 25), for (II) (h,k 0–15, l 0–19). All observations [5186 for (I), 2628 for (II)] were corrected for Lorentz and polarization effects, but not for absorption. Three intensities each were monitored over the course of data collection [(I) $\bar{1}46$, 6,0,10, 6,4,$\bar{1}4$, 93·3 h; (II) 257, $\bar{5}\bar{1}4$, 44$\bar{3}$, 43·7 h]. Intensities showed a nearly linear change of −2·2 (5)% (I) and −0·7 (1·0)% (II); a correction was applied to the data for (I) and symmetry-equivalent data were averaged [R_{int} = 1·3% for (I), 3·2% for (II)]. Omitting systematic absences there were 4758 (I) and 2613 (II) unique intensities. The structures were located with *MULTAN*80 (Main *et al.*, 1980). Non-H-atom positions were refined with their U_{iso}'s by full-matrix least squares minimizing $\sum w(|F_o| - |F_c|)^2$ with unit weights, then with their U_{ij}'s. H-atom positions were calculated and placed 1·0 Å from their attached atom and were assigned B's approximately 1·3 times B_{eq} of

Table 2. *Positions and equivalent isotropic vibrational amplitudes for the non-*H *atoms in* (II), *with e.s.d.'s in parentheses*

$B_{eq} = (8\pi^2/3)\sum_i\sum_j U_{ij} a_i^* a_j^* \mathbf{a}_i.\mathbf{a}_j.$

	x	y	z	B_{eq}(Å^2)
O1	0·4279 (2)	0·5928 (2)	0·728	4·08 (5)
O2	0·3340 (2)	0·7729 (2)	0·7459 (3)	5·45 (6)
O3	0·7714 (2)	0·7579 (2)	0·7331 (2)	3·59 (4)
O4	0·7828 (2)	0·9514 (2)	0·6597 (2)	3·99 (5)
C2	0·4329 (3)	0·7196 (3)	0·7417 (3)	3·71 (7)
C3	0·5523 (3)	0·7763 (3)	0·7493 (2)	3·14 (6)
C4	0·6554 (3)	0·7092 (3)	0·7358 (2)	3·10 (6)
C5	0·7554 (4)	0·5001 (3)	0·7208 (3)	4·45 (8)
C6	0·7400 (4)	0·3734 (3)	0·7148 (4)	5·21 (8)
C7	0·6236 (4)	0·3219 (3)	0·7133 (3)	5·16 (9)
C8	0·5190 (4)	0·3952 (3)	0·7176 (3)	4·54 (8)
C9	0·5341 (3)	0·5223 (3)	0·7235 (3)	3·56 (7)
C10	0·6503 (3)	0·5763 (3)	0·7250 (3)	3·32 (6)
C11	0·5624 (3)	0·9136 (3)	0·7702 (3)	3·34 (6)
C12	0·6865 (3)	0·9338 (3)	0·8209 (3)	3·68 (7)
C13	0·7865 (3)	0·8894 (3)	0·7518 (2)	3·17 (6)
C14	0·9159 (3)	0·9000 (3)	0·7921 (3)	4·54 (8)
C15	0·5615 (3)	0·9882 (3)	0·6770 (3)	3·43 (6)
C16	0·6725 (3)	1·0047 (3)	0·6271 (3)	3·49 (6)
C17	0·6805 (4)	1·0776 (3)	0·5428 (3)	4·45 (8)
C18	0·5721 (4)	1·1343 (3)	0·5100 (3)	5·29 (9)
C19	0·4610 (4)	1·1195 (3)	0·5591 (3)	5·12 (9)
C20	0·4556 (3)	1·0462 (3)	0·6415 (3)	4·38 (8)
C21	0·8020 (5)	1·0962 (4)	0·4902 (4)	6·60 (10)

the adjacent C atom; they were revised as the model improved but not refined. In the latter stages of refinement on (I), difference Fourier maps showed that the acetyl methyl H's were disordered; a local model calculated to best represent the map features required two sets of three H's in each of the staggered conformations with respect to the next adjacent non-H-atom bonds, weighted 0·7 and 0·3. Scattering factors were from *International Tables for X-ray Crystallography* (1974) except for H (Stewart, Davidson & Simpson, 1965). Final agreement factors for (I) $R = 0{\cdot}050$, $wR = 0{\cdot}063$, GOF = 1·50 for 2767 $I \geq 3\sigma(I)$; for (II) $R = 0{\cdot}049$, $wR = 0{\cdot}055$, GOF = 1·29 for 1425 $I \geq 2{\cdot}5\sigma(I)$. Weights corresponding to $1/\sigma(F^2)$ were introduced in the final stages of the refinements on the 236 (I) and 216 (II) variables; scale factors 0·263 (1) (I), 0·282 (2) (II); in the last cycle, variable shifts were less than 0·22 (I) and 0·01 (II) of their estimated e.s.d.'s; final difference map excursions were between +0·24 and −0·19 e Å^{-3} (I) and +0·19 and −0·36 e Å^{-3} (II). Final atom positions and equivalent isotropic vibrational factors for the non-H atoms are given in Tables 1 and 2.* Selected interatom lengths and interbond angles are presented in Table 3. Programs used throughout were from the locally modified Enraf–Nonius *SDP* (Frenz, 1988).

* Lists of anisotropic vibrational amplitudes, H-atom positions and structure factors have been deposited with the British Library Document Supply Centre as Supplementary Publication No. SUP 52856 (45 pp.). Copies may be obtained through The Technical Editor, International Union of Crystallography, 5 Abbey Square, Chester CH1 2HU, England.

Table 3. *Interatom lengths* (Å) *and interbond angles* (°) *for* (I) *and* (II) *with e.s.d.'s in parentheses*

	(I)	(II)		(I)	(II)
O1—C2	1·386 (2)	1·382 (4)	C7—C8	1·376 (3)	1·379 (5)
O1—C9	1·375 (2)	1·377 (4)	C8—C9	1·389 (3)	1·382 (4)
O2—C2	1·203 (2)	1·213 (4)	C9—C10	1·384 (3)	1·382 (4)
O3—C4	1·357 (2)	1·358 (3)	C11—C12	1·531 (3)	1·522 (5)
O3—C13	1·435 (2)	1·450 (3)	C11—C15	1·533 (3)	1·500 (5)
O4—C13	1·455 (3)	1·419 (4)	C12—C13	1·506 (3)	1·509 (4)
O4—C21	1·355 (2)		C13—C14	1·514 (3)	1·504 (4)
O4—C16		1·394 (4)	C15—C16	1·383 (3)	1·388 (4)
O5—C21	1·200 (3)		C15—C20	1·395 (3)	1·389 (4)
C2—C3	1·445 (3)	1·430 (4)	C16—C17	1·393 (3)	1·392 (5)
C3—C4	1·343 (2)	1·339 (4)	C17—C18	1·379 (3)	1·393 (5)
C3—C11	1·509 (2)	1·512 (4)	C17—C21		1·506 (6)
C4—C10	1·446 (2)	1·443 (4)	C18—C19	1·373 (4)	1·380 (6)
C5—C6	1·381 (3)	1·380 (5)	C19—C20	1·393 (3)	1·372 (6)
C5—C10	1·400 (3)	1·402 (5)	C21—C22	1·486 (3)	
C6—C7	1·383 (4)	1·374 (6)			
C2—O1—C9	121·6 (2)	121·3 (2)	C3—C11—C15	114·0 (2)	111·6 (2)
C4—O3—C13	118·5 (1)	118·5 (2)	C12—C11—C15	113·3 (2)	108·1 (2)
C13—O4—C21	120·0 (1)		C11—C12—C13	113·4 (2)	107·6 (3)
C13—O4—C16		119·9 (2)	O3—C13—O4	101·4 (1)	107·7 (2)
O1—C2—O2	116·3 (2)	116·2 (3)	O3—C13—C12	111·1 (2)	109·8 (2)
O1—C2—C3	118·1 (1)	117·9 (3)	O3—C13—C14	104·8 (1)	104·0 (2)
O2—C2—C3	125·5 (2)	125·9 (3)	O4—C13—C12	111·5 (1)	112·3 (2)
C2—C3—C4	119·6 (1)	120·5 (3)	O4—C13—C14	111·6 (2)	108·2 (3)
C2—C3—C11	118·5 (1)	119·8 (3)	C12—C13—C14	115·3 (2)	114·4 (3)
C4—C3—C11	121·8 (2)	119·7 (3)	C11—C15—C16	123·3 (1)	118·4 (3)
O3—C4—C3	124·8 (1)	124·1 (3)	C11—C15—C20	118·5 (2)	122·7 (3)
O3—C4—C10	113·2 (1)	114·7 (3)	C16—C15—C20	118·2 (2)	118·8 (3)
C3—C4—C10	122·0 (2)	121·3 (3)	C15—C16—C17	121·5 (2)	121·9 (3)
C6—C5—C10	119·6 (2)	119·1 (3)	C16—C17—C18	119·6 (2)	117·3 (4)
C5—C6—C7	120·2 (2)	120·7 (4)	C17—C18—C19	119·7 (2)	121·6 (4)
C6—C7—C8	121·1 (2)	121·1 (3)	C18—C19—C20	120·9 (2)	119·8 (4)
C7—C8—C9	118·5 (2)	118·3 (3)	C15—C20—C19	120·1 (2)	120·6 (4)
O1—C9—C8	117·1 (2)	116·8 (3)	O4—C21—O5	124·0 (2)	
O1—C9—C10	121·4 (1)	121·4 (3)	O4—C21—C22	111·0 (2)	
C8—C9—C10	121·5 (2)	121·7 (3)	O5—C21—C22	125·0 (2)	
C4—C10—C5	123·8 (2)	123·8 (3)	O4—C16—C15		121·9 (3)
C4—C10—C9	117·1 (2)	117·1 (3)	O4—C16—C17		116·2 (3)
C5—C10—C9	119·0 (2)	119·1 (3)	C16—C17—C21		121·3 (4)
C3—C11—C12	108·2 (1)	106·8 (2)	C18—C17—C21		121·4 (3)

The correct enantiomorph for the space group in which (II) occurs was deduced from the likely absolute configuration of (II). Optical rotations of warfarin and its phenyl-substituted analogs derived from the less-soluble (+)-quinidine salts are levorotatory. This suggests, by analogy to warfarin (West, Preis, Schroeder & Link, 1961; Valente, Trager & Jensen, 1975), that the dihydropyranyl 4-position has the *S* absolute configuration. This assignment is strengthened by the circular dichroism (CD) spectrum of (II). After diffraction experiments were complete, the data crystal of (II) was dissolved in acetonitrile and its CD spectrum recorded on a Jasco 500-A Spectropolarimeter over the range 195–350 nm. The sample showed negative Cotton effects at 305 and 220 nm, and positive effects at 270, 242 and 202 nm. The positions and intensities of the bands are consistent with the assignment of 2*S*,4*S* absolute configuration to (II) (Valente & Trager, 1978), and hence the space-group enantiomorph given above.

Factor analysis

A search for systematic structural changes in warfarin derivatives differing in the nature of the

ketal leaving group was conducted on six structures, including the two reported here, by multivariate principal component analysis. The method, widely employed in the social sciences, analyzes covariances or correlations in a set of possibly interrelated variables and attempts to account for most of the variance in the data set with a few 'factors'. Application to chemical systems has been described by Murray-Rust (1982). Routines employed were those in the *SPSS* (Norusis, 1986).

Three warfarin hemiketal structures [(III), Bravic, Gaultier & Hauw (1973); (IV), Csoregh & Edstrom (1976); (V), Valente, Trager & Jensen (1975)], a 2-O-aryl warfarin [(VI), Ruggiero, Valente & Eggleston (1989*a*)] closely related to (II), the 2-O-aryl warfarin (II) and the 2-O-acyl warfarin (I) structures described here comprise the analyzed group. Final agreement factors (R_F) for each are less than 0·054 [except (IV), 0·086] on counter-collected data; least-squares refinements included all non-H atoms and anisotropic vibrational terms; H-atom contributions were included. Each structure contains an axial dihydropyranyl (hemi)ketal fragment (see the scheme below). Eleven structural parameters chosen for analysis include those for the ketal and the ring unsaturation since the two features are adjacent; they are the bond lengths r_x (exocyclic ketal C—O), r_n (endocyclic ketal C—O), r_f (endocyclic =C—O) and r_e (endocyclic C=C), and the inter-bond angles α_1 (endocyclic at O), α_2 (endocyclic at ketal C), α_6 [endocyclic at C(sp^2) adjacent to O], β (exocyclic O—C—O), and the torsions τ_f (intraring at r_f), τ_a (intraring at r_n) and τ_x (C—O—C—O). The pK_a of the conjugate acid of the leaving group was variously included in trials to identify the variables with which it is most closely correlated. Values are listed in Table 4, means and standard deviations are given in Table 5. The bond lengths and angles used are uncorrected values from the X-ray structure determinations and as such, they bear the built-in biases typical in room-temperature structures with the assumption of atomic spherical electron density distributions, *etc.* The values are inaccurate in detail, but the trends in the lengths and angles are preserved since for the most part the nature and magnitude of the systematic inadequacies of the models are common to the structures. Angle measures are converted to radians and normalized ($\theta = \bar{r}\theta\pi/180$) by the mean length of the angle arms; torsions similarly by the mean length of the dihedral arms.

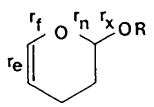

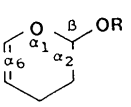

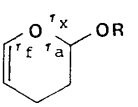

Factor analysis was applied to the covariance and correlation matrices for models with varying numbers of the 11 structural features. In the main, two principal components emerge to account for most of the parameter variance. Factor extraction was gauged as reasonable through the Kaiser–Meyer–Olkin index (0·60–0·90′ s). Residual correlation matrices, *i.e.* one of differences between the matrix of covariances and those produced from the factor model, always had fewer than 10% of terms exceeding 0·05. Various factor rotation treatments with orthogonal or oblique eigenvector extractions gave similar, consistent interpretations of the principal factors responsible for the structural variances. The 11-parameter model, discussed below, gave representative results.

Table 4. *Selected structural parameters of six axial dihydropyranyl (hemi) ketals*

Common configurations were employed for the six structures.

	—O*R*	pK_a	r_x (Å)	r_n (Å)	r_f (Å)	r_e (Å)
(I)	—OAc	4·7	1·455 (3)	1·435 (2)	1·357 (2)	1·343 (2)
(II)	—OAr	9·9	1·419 (4)	1·450 (3)	1·358 (3)	1·339 (4)
(III)	—OH	15·7	1·383 (4)	1·474 (3)	1·347 (3)	1·362 (3)
(IV)	—OH	15·7	1·388 (4)	1·460 (5)	1·345 (5)	1·361 (6)
(V)	—OH	15·7	1·385 (3)	1·483 (2)	1·351 (2)	1·351 (3)
(VI)	—OAr	9·9	1·426 (5)	1·448 (4)	1·338 (4)	1·370 (6)

	α_1 (°)	α_2 (°)	α_6 (°)	β (°)
(I)	118·5 (1)	111·1 (2)	124·8 (1)	101·4 (1)
(II)	118·5 (2)	109·8 (2)	124·1 (3)	107·1 (2)
(III)	116·8 (3)	107·6 (3)	124·2 (3)	108·7 (3)
(IV)	117·3 (3)	108·0 (3)	124·0 (3)	109·3 (3)
(V)	115·6 (2)	108·2 (2)	124·7 (2)	108·0 (2)
(VI)	120·4 (3)	110·5 (3)	123·9 (4)	107·1 (3)

	τ_f (°)	τ_a (°)	τ_x (°)	τ_{OCOR} (°)
(I)	6·6 (3)	−34·4 (2)	84·2 (2)	−173·6 (2)
(II)	−3·9 (4)	−30·1 (4)	92·4 (3)	97·0 (3)
(III)	13·1 (7)	−44·2 (5)	72·4 (7)	−65·7 (18)
(IV)	13·5 (5)	−44·3 (4)	71·4 (4)	−59·1 (67)
(V)	14·1 (2)	−46·2 (2)	71·1 (2)	−81·9 (16)
(VI)	1·1 (5)	27·7 (4)	93·3 (4)	92·0 (3)

Table 5. *Means and standard deviations of structural parameters used in factor analysis*

Common configurations were employed for the six structures.

	Distances (Å)	Angles (°)
r_x	1·409 (29)	
r_n	1·458 (18)	
r_f	1·349 (8)	
r_e	1·354 (12)	
α_1	2·887 (41)	117·8 (7)
α_2	2·830 (38)	109·2 (6)
α_6	2·933 (9)	124·3 (3)
β	2·678 (72)	107·0 (12)
τ_f	0·173 (195)	7·0 (79)
τ_a	−0·944 (202)	−37·8 (81)
τ_x	1·945 (254)	80·8 (105)

Discussion

The structures

Ellipsoid plots of the molecular structures of (I) and (II) are given in Figs. 1 and 2. The numbering scheme shown is based on the coumarin system,

considered central to the class of coumarin anticoagulant drugs of which warfarins are examples. Bond lengths and angles (Table 3) are similar to each other and typical of warfarin stuctures except for the variations within the ketal. Each molecule contains an embedded dihydropyran ring [labelled O(3)—C(13)—C(12)—C(11)—C(3)=C(4)]. The structure of the aryl ketal (II) requires that the phenyl substituent on this ring [at C(11)] be disposed pseudoaxially because its 2′-O atom [O(4)] links with the ring at the ketal C atom [C(13)]. This *cis* arrangement necessarily occurs during the intramolecular dehydration of 2′-hydroxy-3′-methylwarfarin, the precursor to (II). In the synthesis of the 2-O-acylwarfarin (I), there are no constraints favoring the formation of either the *cis* or the *trans* isomer. The form isolated from the rapidly quenched reaction mixture happens to have the phenyl [at C(11)] and the acetoxy [at C(13)] groups on the embedded dihydropyran ring oriented *cis* to each other.

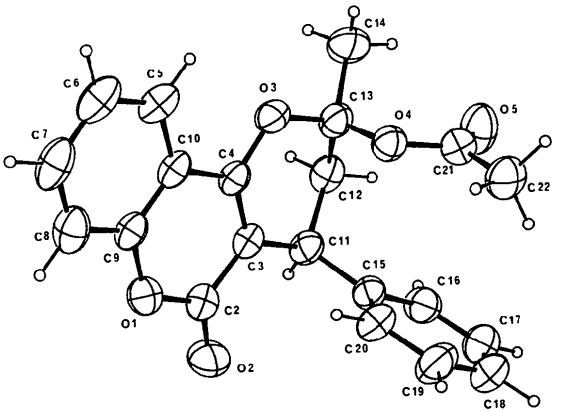

Fig. 1. An *ORTEP* (Johnson, 1976) plot of the structure of (I) with numbering following the coumarin ring; 50% probability ellipsoids are shown for the non-H atoms.

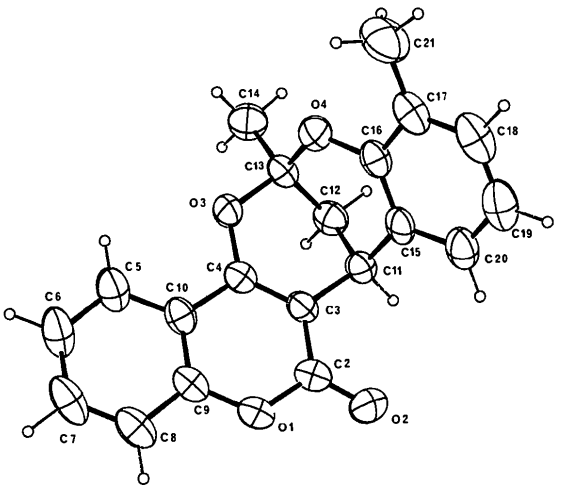

Fig. 2. A plot of the structure of (II).

Thus while both (I) and (II) have phenyls disposed pseudoaxially, their ring planes are oriented differently in the two structures. In (I), the phenyl and acetoxy groups are roughly aligned; their mean planes through the non-H atoms are inclined by 19° to each other. There are several nonbonded atomic contacts between these groups at distances between 3·28 and 3·81 Å, suggesting that favorable nonbonded interactions are in part responsible for this arrangement. The phenyl ring is disposed nearly perpendicular to the mean plane of the coumarin ring. In (II), the phenyl group is rotated approximately 81° about C(11)—C(15) compared with (I) because of its covalent link to the 2-O atom on the dihydropyran ring (see Fig. 1).

In the general structure of the warfarin hemiketals and methyl ketals, 2-O-substituents are disposed *exo* to the dihydropyran ring and synclinal to the ring O atom [torsion angle O—C—O—H(C); −60 to −80°]. This arrangement is commonly associated with the exoanomeric effect in sugars. Ketals (I) and (II), in contrast, have different conformations. Of course, in (II) the 2-O-phenyl must lie over the dihydropyran ring to make the 1,3-diaxial link; and the O(3)—C(13)—O(4)—C(16) torsion angle is +97·0 (3)°. In (I), the 2-O-acetyl group is found *trans* to the endocyclic ketal C—O with the O(3)—C(13)—O(4)—C(21) torsion angle −173·6 (2)°.

The dihydropyran rings in each structure adopt half-chair conformations distorted towards the *e,f*-diplanar forms (Valente, Santarsiero & Schomaker, 1979). Ring-displacement asymmetry parameters ΔC_2 for the dihydropyran rings are 0·051 (1) (I) and 0·130 (1) (II) (Nardelli, 1983). The latter value effectively represents a *sofa* conformation like that found in the related structure of cyclic dehydrated 2′-hydroxywarfarin (Ruggiero, Valente & Eggleston, 1989*a*), but the conformation is not more distorted than some found in unconstrained warfarin (hemi)-ketals (Valente, Eggleston & Schomaker, 1987). Differences between the ketal portions of the molecular structures of (I) and (II), and between these and other warfarin structures are of particular interest. Selected structural features for warfarin hemiketals [(III)–(V)], aryl ketals [(II), (VI)] and the acyl ketal (I) are gathered in Table 4.

The most striking trend to be found in this short series of related molecules is the variation in the length of the endocyclic (r_n) and exocyclic (r_x) ketal C—O bonds. Since the ketal C atom is C(13), r_n is C(13)—O(3) and r_x is C(13)—O(4). In the acyl ketal (I) these lengths are 1·435 (2) and 1·455 (2) Å, and in the aryl ketal (II), they are 1·450 (3) and 1·419 (4) Å, respectively. In each case, r_n is shorter than that found in the hemiketals [(III)–(V), 1·472 Å, $N = 3$], and r_x is longer. An explanation for this may be found by considering likely contributions to the

dihydropyran ground-state structure (*A*) from extreme resonance form (*B*) (see the scheme below). Since both 2-aryloxy and acyloxy may be considered to be superior leaving groups compared to hydroxide, they each would have a greater contribution to the ground state from structure (*B*), tending to shorten r_n and lengthen r_x.

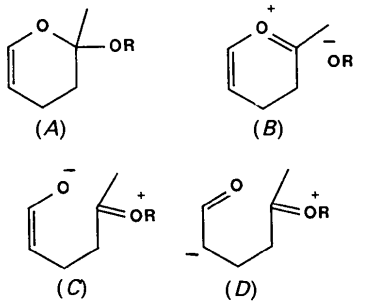

To test the semiquantitative dependence of the leaving-group tendencies upon the bonding in warfarin (hemi)ketals requires just such a range of substituents as is represented in Table 4. In the short series, 2-O-substituents are present for which the conjugate acids to the exocyclic leaving groups differ by 11 pK units. (The hemiketal structures are *trans*-2-hydroxy-4-phenyl compounds and show intermolecular hydrogen bonding; the pK_a is taken as 15·7.) A plot of the pK_a of the conjugate acids to 2-O-substituents against the C—O lengths in this series is shown in Fig. 3. (For comparison, the relationships found in the tetrahydropyranyl acetals are also given in the figure.) The lengths of both r_x and r_n appear as functions of the exocyclic leaving-group tendencies. The resultant linear free-energy relationship in these α-dihydropyranyl ketals is similar to that found for the α-tetrahydropyranyl acetals (Jones & Kirby, 1984), and the slopes agree to within 7%. The exocyclic r_x bond relationship among the dihydropyranyl ketals is:

$$r_x = 1{\cdot}485 - (6{\cdot}350 \times 10^{-3}) \times \mathrm{p}K_a(R\mathrm{OH}),$$

and the r_n bond follows:

$$r_n = 1{\cdot}416 + (3{\cdot}538 \times 10^{-3}) \times \mathrm{p}K_a(R\mathrm{OH}).$$

Examination of Fig. 3 shows that the crossover point for the acetal series, *i.e.* the pK_a at which the C—O bonds have equal length, is 1·41 Å, and for leaving groups for which the conjugate acids have pK_a = 12·7. In the warfarin α-dihydropyranyl ketals, the crossover occurs at C—O length 1·44 Å and at about pK_a = 7·0. This difference may be ascribed to the dissimilarity between the saturated and unsaturated rings and their implied leaving-group tendencies in comparison with the exocyclic groups. Consider the model in which enolate is an endocyclic leaving group in dihydropyran ketals as represented by resonance structure (*C*). Since enolate basicity is about six orders of magnitude weaker than a primary alkoxide, the endocyclic leaving group in tetrahydropyranyl acetals, r_n is correspondingly longer. Structures (*B*) and (*C*) then describe opposing extremes in spontaneous ketal cleavage of either O substituent, and ground-state structures are influenced by the difference in the basicities of the potential leaving groups. For comparable exocyclic leaving groups in α-tetrahydropyranyl acetals and α-dihydropyranyl ketals, the latter have longer r_n and shorter r_x, and ground-state structures relatively more distorted toward endocyclic ketal cleavage [(*A*) + (*C*)].

Factor analysis

The observed trends in C—O bond lengths are part of a more extensive and chemically meaningful scheme of ketal cleavage. Table 6 shows the results of the analysis of the variable correlations or covariations of the structural parameters associated with the ketal group and adjacent portions of the dihydropyran ring. Two factors account for 87·1% of the total variance in an 11-parameter model. A third factor accounts for 10% of the variance, an amount typical of the variance in any parameter. No physically meaningful interpretation appears to be attached to it. Other factors are even less statistically important by comparison.

Factor 1 in the analysis corresponds to a trend indicative of the early stages of exocyclic ketal cleavage like the unimolecular dissociation (*E*1) of the ketal toward an intimate ion pair. Components associated with this trend are the lengthening of r_x, shortening of r_n, and widening of intraring angles at the ring O and the ketal C. Additionally, a declining

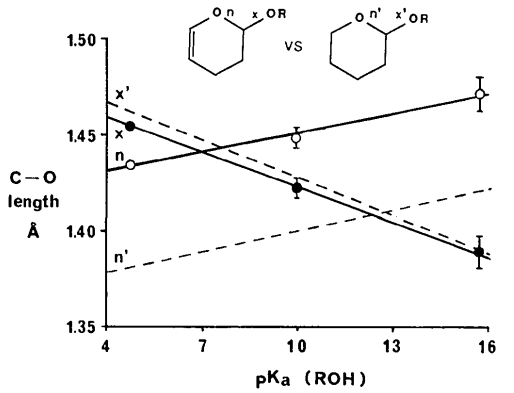

Fig. 3. A graph of C—O bond lengths in dihydropyranyl ketals from warfarin derivatives as a function of the pK_a of the conjugate acid of the exocyclic ketal leaving group (solid lines). For comparison, C—O bond lengths for tetrahydropyranyl acetals are also shown (dashed lines, see text).

Table 6. *Factors extracted from* 11*-variable analysis*

	Factor 1	Factor 2	Factor 3
% of Variance	59	28	10
Eigenvalues (unit variance)	6·477	3·089	1·099
Eigenvalues (Å²)	0·08974	0·04280	0·01522
Matrix of factor correlations with variables*			
r_x	**0·939**	−0·245	0·237
r_n	**−0·916**	0·027	−0·162
α_1	**0·861**	0·489	0·124
α_2	**0·966**	−0·120	0·187
τ_a	**0·941**	0·284	−0·138
τ_f	**−0·859**	−0·283	0·403
τ_x	**0·923**	0·261	−0·225
β	−0·670	0·587	−0·447
r_e	−0·319	**0·805**	0·491
r_f	0·231	**−0·854**	−0·447
α_6	−0·049	**−0·908**	0·306

* Highly correlated factor components are given in bold type.

intraring torsion τ_f and increasing τ_a indicate dihydropyran ring flattening, and the increasing C—O_n—C—O_x torsion τ_x agrees with a model for incipient conjugate base (^-OR) elimination. In short, factor 1 describes an increasing participation of structure *B* in the ground state of the dihydropyranyl ketals. It correlates well with decreasing pK_a of the conjugate acid of the leaving group, and accounts for 59% of the variance in the model group. Such a model bears a resemblance to the mechanism for acid-catalyzed hydrolysis of acetals and ketals. It is the C—O*R* bond which cleaves after protonation (*A*1 mechanism) and the solution hydrolysis rates are considerably increased by the ability of the substituent to remove charge as indicated by the negative reaction constants typically observed (Isaacs, 1987).

A second factor can be extracted which principally involves features not related to ketal cleavage. The C=C and the adjacent =C—O lengths are inversely correlated, and the intervening angle opens as C=C shortens. Leaving-group basicity is poorly correlated with this factor. Since the dihydropyran ring unsaturation is part of, and conjugated with, the benzopyranone (coumarin) system, various plausible resonance contributions in the coumarin can bear on the location of the C atom central to the C=C—O group. These appear to be dependent on specific crystalline environments and intermolecular contacts.

The dihydropyran ring

Returning to the C—O bond variations, functions for the r_n lengths in both the saturated and unsaturated systems agree remarkably well (Fig. 3). The effectiveness of the anomeric $n_O \rightarrow \sigma^*$(C—O) on r_x variability in the ketals, in which the ketal C atom has four bonds to non-H atoms, is similar to that observed in the acetals. However, the r_n bonds are 0·052 Å longer for the α-dihydropyranyl ketals than in the saturated acetals. This feature primarily arises from the increased electron demand of an incipient intraring enolate leaving group relative to the exocyclic ketal substituent. The endocyclic C(sp^3)—O length in unsubstituted and unconjugated dihydropyran is itself a naturally longer bond ($\simeq$1·45 Å) as suggested by the C—O lengths in aryl and vinyl ethers (Allen & Kirby, 1984). The effect is seen in the warfarin hemiketals and in the structure of deoxywarfarin (Ruggiero, Valente & Eggleston, 1989*b*). In deoxywarfarin, a 'zero substituent' case in which an axial —H takes the place of exocyclic —O*R*, the endocyclic C(sp^3)—O is 1·472 (4) Å. This is essentially indistinguishable from the warfarin hemiketals (Table 4) which have the least basic (poorest leaving group) ketal substituents as suggested in (*C*, *R* = H). In both cases, the exocyclic substituent is a poor competitor against the intraring enolate. Other structures of non-anomeric dihydropyran-type compounds provide similar evidence. A variety of chroman structures related to Dianin's compound (Flippen, Karle & Karle, 1970; Hardy, McKendrick, MacNicol & Wilson, 1979; Gall, Hardy, McKendrick & MacNicol, 1979), which lack a 2-O-substituent, show elongated endocyclic C(sp^3)—O bonds [1·46 (1) Å, *N* = 5]. Proton nuclear magnetic resonance data on dihydropyran show a relatively high-field resonance for H in the sequence O—C=C—H. An explanation has been advanced which invokes participation of structures like (*D*) (Bushweller & O'Neill, 1969). Also, the slightly higher pseudorotational barrier in dihydropyran compared to cyclohexene (Anet & Haq, 1965) may be a consequence of the somewhat stiffer =C—O bond which contributions from (*D*) would foster. At present, more detail on simple dihydropyran systems is not available. The microwave spectrum (Lopez & Alonso, 1985) of dihydropyran was fitted to a model that assumed most of the non-conformationally variable structural features.

The r_n bonds in warfarin dihydropyranyl ketals are longer than in simple dihydropyrans since the enolates (*D*) are almost certainly even stronger bases through conjugation with a distant electron sink (coumarin carbonyl O). While warfarin derivatives lacking this extended conjugation have not been characterized, chroman structures without a distant terminal O atom conjugated with the chroman dihydropyran have been studied [see above and Cannon, McDonald, Sierakowski, White & Willis (1975) and Jones, Kennard & Sheldrick (1977)] and have slightly shorter C(sp^3)—O lengths (1·46 Å, *N* = 7) than those which are conjugated [1·485 (15) Å, *N* = 15, various dihydropyran ring conformations] (Begley, Crombie, Slack & Whiting, 1977*a*,*b*; Ghisalberti, Jeffries, Raston, Skelton, White & Worth, 1981; Ghisalberti, Jeffries, Raston, White &

Stuart, 1981). The intervening bond lengths are normal.

The incipient reaction

The range of structures is crudely represented as lying on the reaction path (*C*)–(*A*)–(*B*). When the leaving group (O*R*) is poor, such as in the warfarin hemiketals (O*R* = OH), the contribution from (*C*) is important, which amounts to ring opening and formation of the open-chain keto warfarin isomer. Open warfarin isomers are known from NMR studies in relatively non-polar solvents ($CDCl_3$) to constitute 15–75% of the equilibrium mixture dynamically occurring between the open and diastereomeric cyclic hemiketal forms (Valente, Lingafelter, Porter & Trager, 1977; Valente & Hodgson, 1979). In the cases in which the leaving groups are less basic, contributions from (*B*) are increasingly important, which is a model for *E*1-like elimination with respect to (*A*). The same in solution could lead to ketal hydrolysis, since the first stages of *E*1 and S_n1 reactions are similar. Both reactions are well known for warfarin derivatives but the elimination appears to be more important as the leaving-group basicity decreases. Thus, warfarin methyl ketals are slowly hydrolyzed in acidic aqueous acetone at 310 K (Bush & Trager, 1983), probably through structures more like (*C*) than (*B*). Dehydration of warfarin hemiketal to the 4*H*-pyrano derivative requires refluxing benzene for 8 h over P_2O_5 (Chan, Lewis & Trager, 1972). Warfarin can also be dehydrated through the activated ethanoylwarfarin (I), which eliminates acetic acid in 5 min at room temperature in acetic anhydride with a small amount of $HClO_4$ (Seidman, Robertson & Link, 1950).

This work has been supported in part by a grant from the Mississippi Affiliate of the American Heart Association (MS-86-G-10). Instrumentation grants USE-8950385 and USE-8851694 from the National Science Foundation are gratefully acknowledged.

References

ALLEN, F. H. & KIRBY, A. J. (1984). *J. Am. Chem. Soc.* **106**, 6197–6200.

ANET, F. A. L. & HAQ, M. Z. (1965). *J. Am. Chem. Soc.* **87**, 3147–3153.

BEGLEY, M. J., CROMBIE, L., SLACK, D. A. & WHITING, D. A. (1977*a*). *J. Chem. Soc. Perkin Trans.* 1, pp. 2393–2402.

BEGLEY, M. J., CROMBIE, L., SLACK, D. A. & WHITING, D. A. (1977*b*). *J. Chem. Soc. Perkin Trans.* 1, pp. 2402–2410.

BRAVIC, G., GAULTIER, J. & HAUW, C. (1973). *C. R. Acad. Sci. Ser. C*, **277**, 1215–1218.

BRIGGS, A. J., GLENN, R., JONES, P. G., KIRBY, A. J. & RAMASWAMY, P. (1984). *J. Am. Chem. Soc.* **106**, 6200–6206.

BÜRGI, H.-B. & DUBLER-STEUDLE, K. C. (1988). *J. Am. Chem. Soc.* **110**, 7291–7299.

BÜRGI, H.-B. & DUNITZ, J. D. (1983). *Acc. Chem. Res.* **16**, 153–161.

BUSH, E. & TRAGER, W. F. (1983). *J. Pharm. Sci.* **72**, 830–831.

BUSHWELLER, C. H. & O'NEILL, J. W. (1969). *Tetrahedron*, **53**, 4713–4716.

CANNON, J. R., MCDONALD, I. A., SIERAKOWSKI, A. F., WHITE, A. H. & WILLIS, A. C. (1975). *Aust. J. Chem.* **28**, 57–62.

CARTER, S. D. & WALLACE, T. W. (1983). *Synthesis*, pp. 1000–1003.

CHAN, K. K., LEWIS, R. J. & TRAGER, W. F. (1972). *J. Med. Chem.* **15**, 1265–1270.

CSOREGH, I. & EDSTROM, S. (1976). *Chem. Commun. Univ. Stockholm*, **4**, 1–20.

FLIPPEN, J. L., KARLE, J. & KARLE, I. (1970). *J. Am. Chem. Soc.* **92**, 3749–3755.

FRENZ, B. A. (1988). *Structure Determination Package*. Enraf–Nonius, Delft, The Netherlands.

GALL, J. H., HARDY, A. D. U., MCKENDRICK, J. J. & MACNICOL, D. D. (1979). *J. Chem. Soc. Perkin Trans.* 2, pp. 376–380.

GHISALBERTI, E. L., JEFFRIES, P. R., RASTON, C. L., SKELTON, B. W., WHITE, A. H. & WORTH, G. K. (1981). *J. Chem. Soc. Perkin Trans.* 2, pp. 577–582.

GHISALBERTI, E. L., JEFFRIES, P. R., RASTON, C. L., WHITE, A. H. & STUART, A. D. (1981). *J. Chem. Soc. Perkin Trans.* 2, pp. 583–589.

HARDY, A. D. U., MCKENDRICK, J. J., MACNICOL, D. D. & WILSON, D. R. (1979). *J. Chem. Soc. Perkin Trans.* 2, pp. 729–734.

IKAWA, M., STAHMANN, M. & LINK, K. P. (1944). *J. Am. Chem. Soc.* **66**, 902–906.

International Tables for X-ray Crystallography (1974). Vol. IV. Birmingham: Kynoch Press. (Present distributor Kluwer Academic Publishers, Dordrecht.)

ISAACS, N. A. (1987). *Physical Organic Chemistry*. New York: Wiley.

JOHNSON, C. K. (1976). *ORTEP*II. Report ORNL-5138. Oak Ridge National Laboratory, Tennessee, USA.

JONES, P. G., KENNARD, O. & SHELDRICK, G. M. (1977). *Acta Cryst.* B**32**, 1982–1987.

JONES, P. G. & KIRBY, A. J. (1984). *J. Am. Chem. Soc.* **106**, 6207–6212.

LOPEZ, J. C. & ALONSO, J. L. (1985). *Z. Naturforsch. Teil A*, **40**, 913–919.

MAIN, P., FISKE, S. J., HULL, S. E., LESSINGER, L., GERMAIN, G. DECLERCQ, J.-P. & WOOLFSON, M. M. (1980). *MULTAN*80. *A System of Computer Programs for the Automatic Solution of Crystal Structures from X-ray Diffraction Data*. Univs. of York, England, and Louvain, Belgium.

MURRAY-RUST, P. (1982). *Acta Cryst.* B**38**, 2818–2825.

NARDELLI, M. (1983). *Acta Cryst.* C**39**, 1141–1142.

NORUSIS, M. J. (1986). *Statistical Package for the Social Sciences*. Chicago: SPSS Inc.

RUGGIERO, G., VALENTE, E. J. & EGGLESTON, D. S. (1989*a*). *Acta Cryst.* C**45**, 1182–1184.

RUGGIERO, G., VALENTE, E. J. & EGGLESTON, D. S. (1989*b*). *Acta Cryst.* C**45**, 1369–1372.

SEIDMAN, M., ROBERTSON, D. N. & LINK, K. P. (1950). *J. Am. Chem. Soc.* **72**, 5193–5195.

STEWART, R. F., DAVIDSON, E. R. & SIMPSON, W. T. (1965). *J. Chem. Phys.* **42**, 3176–3187.

SUTTON, L. E. (1965). *Tables of Interatomic Distances and Configuration in Molecules and Ions*, Special Publication 18. London: The Chemical Society.

VALENTE, E. J., EGGLESTON, D. S. & SCHOMAKER, V. (1987). *Acta Cryst.* C**43**, 533–536.

VALENTE, E. J. & HODGSON, D. J. (1979). *Acta Cryst.* B**35**, 3099–3101.

VALENTE, E. J., LINGAFELTER, E. C., PORTER, W. R. & TRAGER, W. F. (1977). *J. Med. Chem.* **20**, 1489–1493.

VALENTE, E. J., SANTARSIERO, B. D. & SCHOMAKER, V. (1979). *J. Org. Chem.* **44**, 798–802.
VALENTE, E. J. & TRAGER, W. F. (1978). *J. Med. Chem.* **21**, 141–143.
VALENTE, E. J., TRAGER, W. F. & JENSEN, L. H. (1975). *Acta Cryst.* B**31**, 954–960.
WEST, B. D., PREIS, S., SCHROEDER, C. & LINK, K. P. (1961). *J. Am. Chem. Soc.* **83**, 2676–2679.

Acta Cryst. (1990). B**46**, 637–643

Low-Resolution Models for Ribosomal Particles Reconstructed from Electron Micrographs of Tilted Two-Dimensional Sheets

BY Z. BERKOVITCH-YELLIN

Department of Structural Chemistry, Weizmann Institute of Science, Rehovot, Israel, and Max-Planck-Institute for Molecular Genetics, D-1000 Berlin 33, Federal Republic of Germany

H. G. WITTMANN

Max-Planck-Institute for Molecular Genetics, D-1000 Berlin 33, Federal Republic of Germany

AND A. YONATH

Department of Structural Chemistry, Weizmann Institute of Science, Rehovot, Israel, and Max-Planck-Research Unit for Structural Molecular Biology, D-2000 Hamburg 52, Federal Republic of Germany

(*Received* 17 *July* 1989; *accepted* 20 *March* 1990)

Abstract

Models of the whole ribosome (70S) and its large subunit (50S) were obtained at low resolution (47 and 28 Å respectively) by three-dimensional image reconstruction using diffraction data collected from electron micrographs of two-dimensional ordered arrays. The comparison of the various reconstructed images, using interactive computer graphics, enabled the assessment of the reliability of the method, the derivation of the shape of the small subunit (30S) and the assignment of several functional features such as the probable path taken by the nascent protein chain, the presumed site for the process of biosynthesis of proteins, and a feasible mode for tRNA binding. The reconstructed models of the various ribosomal particles may be used for phasing of X-ray diffraction data at low resolution.

Introduction

Structural information is essential for a detailed understanding of the mechanisms of biological processes. The biosynthesis of proteins requires several enzymatic and recognition processes which take place on the ribosomes, the cell organelles where the genetic information is translated into polypeptide chains. The ribosomes are built of two subunits of unequal size which associate upon initiation of protein synthesis. The molecular weights of bacterial ribosomes and their large and small subunits are $2{\cdot}3 \times 10^6$, $1{\cdot}45 \times 10^6$ and $8{\cdot}5 \times 10^5$ daltons and their sedimentation coefficients 70S, 50S and 30S, respectively. The ribosomes are complex assemblies with no internal symmetry, composed of several strands of RNA and a large number of different proteins. A typical large subunit of ribosomes from bacterial sources contains 34–36 different proteins and two RNA chains; the small one is composed of 21 proteins and one RNA chain.

The large size of ribosomal particles, which is an obstacle for crystallographic studies, permits their investigation by electron microscopy. In fact these two techniques may complement each other in structural studies on assemblies with the size of ribosomes: electron microscopy, combined with image reconstruction using Fourier methods, should lead to the determination of the overall shape of the whole ribosome as well as its subunits. These, in turn, may serve as starting models for rotation and translation searches, using X-ray data, aimed at the establishment of the location and orientation of the particles within their respective crystal lattice, information which is most valuable for extracting initial phases at low resolution.

The images of 70S and 50S ribosomal particles from *B. stearothermophiles* were reconstructed at 47 and 28 Å resolution respectively, using data obtained from the diffraction patterns of electron micrographs from two or more tilt series of two-dimensional

0108-7681/90/050637-07$03.00 © 1990 International Union of Crystallography